

# Gene and Linda Voiland School of Chemical Engineering and Bioengineering

## A Microfluidic Platform for Electrochemical Concentration and Detection of Lanthanides and Actinides

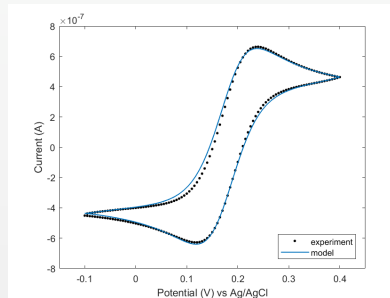
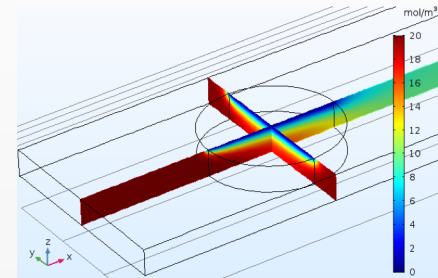
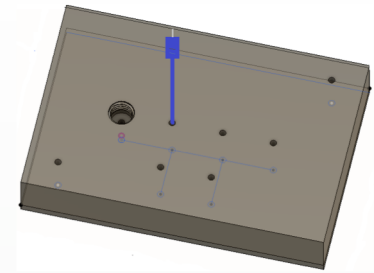
C. F. Ivory, D. E. Molina, A. Medina, H. Beyenal  
Washington State University, Pullman WA 99164





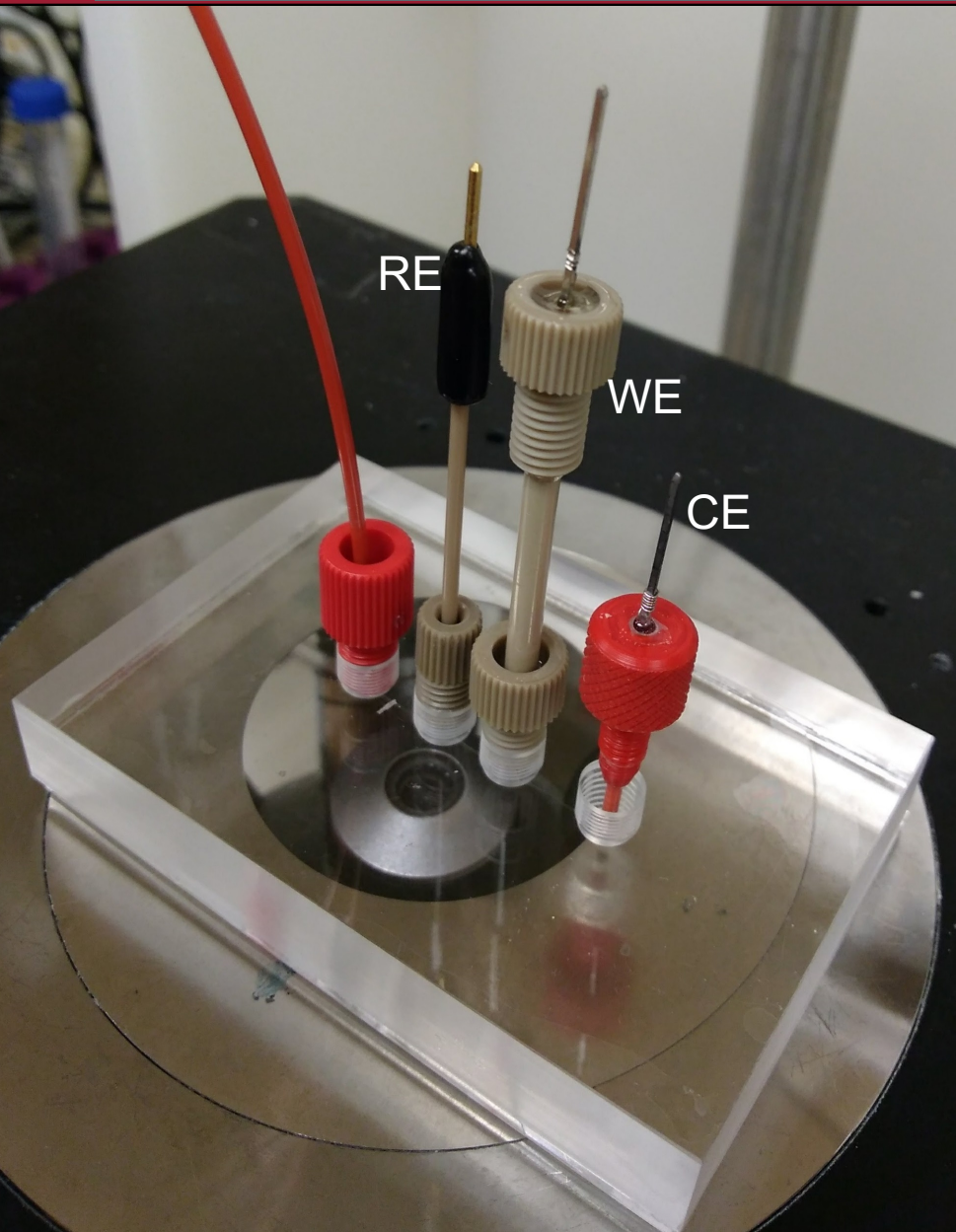
# Outline

- Motivation
- Chip and microelectrode fabrication
- Finite element simulation
- Comparison with experiments
- Conclusions





# Microfluidic Chip & Electrodes



Mold: SU-8 photo resist layer on Polyethyleneimine (PEI) substrate  
std. photolithography

Hot embossed  $150 \times 20 \mu\text{m}$  channel

Poly(methyl methacrylate) (PMMA):  
1.  $1/8$ " channel coupon  
2.  $5/16$ " ports coupon

Monolithic threaded ports (CNC-machined)

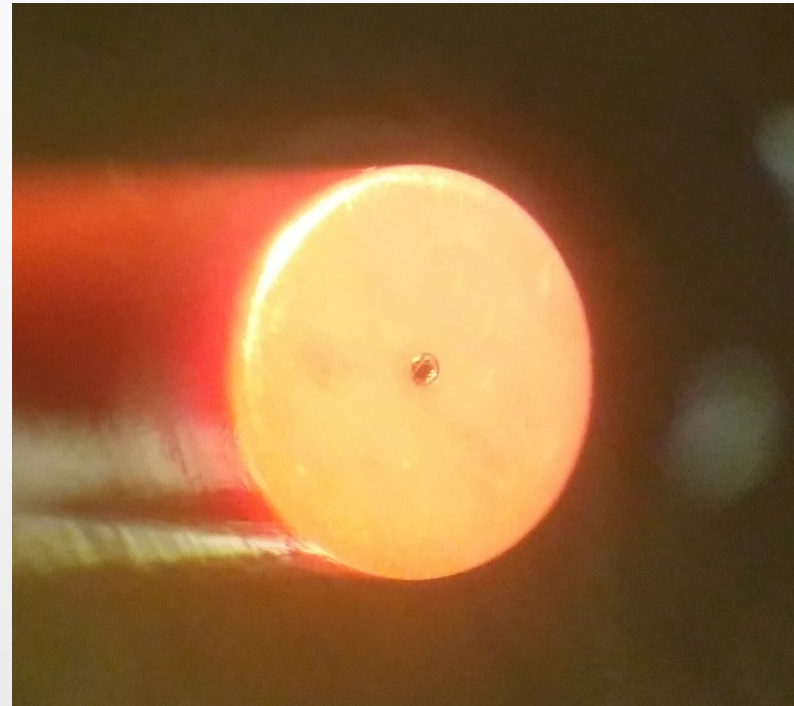
IPA solvent bonding (low T & P)



# Microfluidic Chip & Electrode

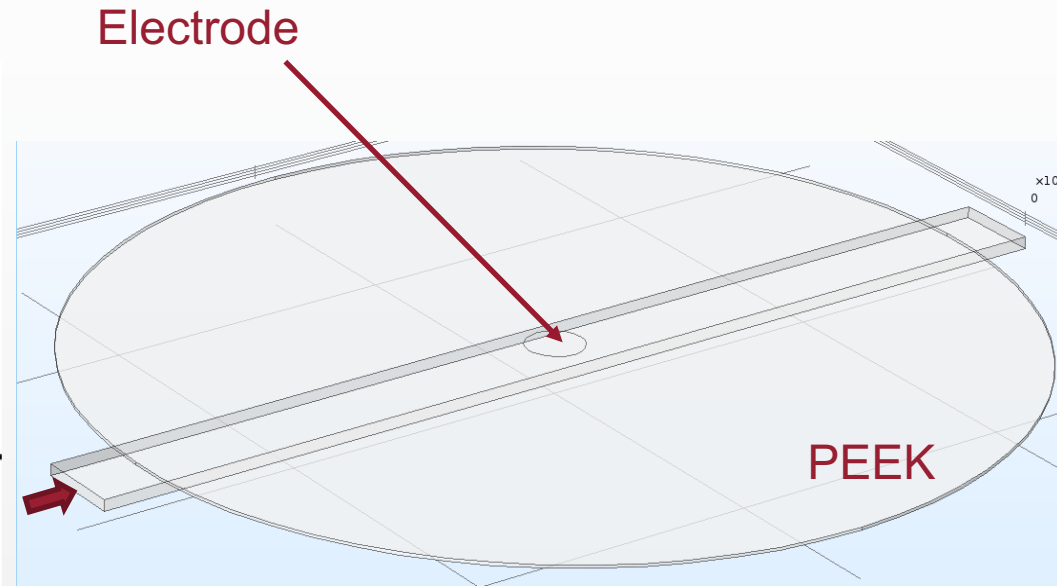
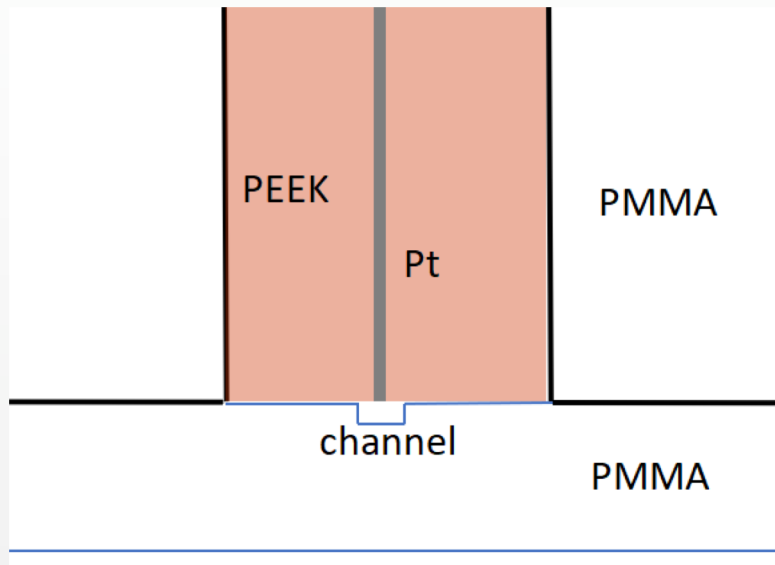
## Working Electrode – Pt microdisc

- PEEK tubing: inert, strong, biocompatible
- Dual tubing (1/16"-1/8" OD) for strength
- Pt-100  $\mu\text{m}$  wire (125  $\mu\text{m}$  ID tubing)
- Slow curing epoxy sealant
- Removable, polishable
- Electrode centered



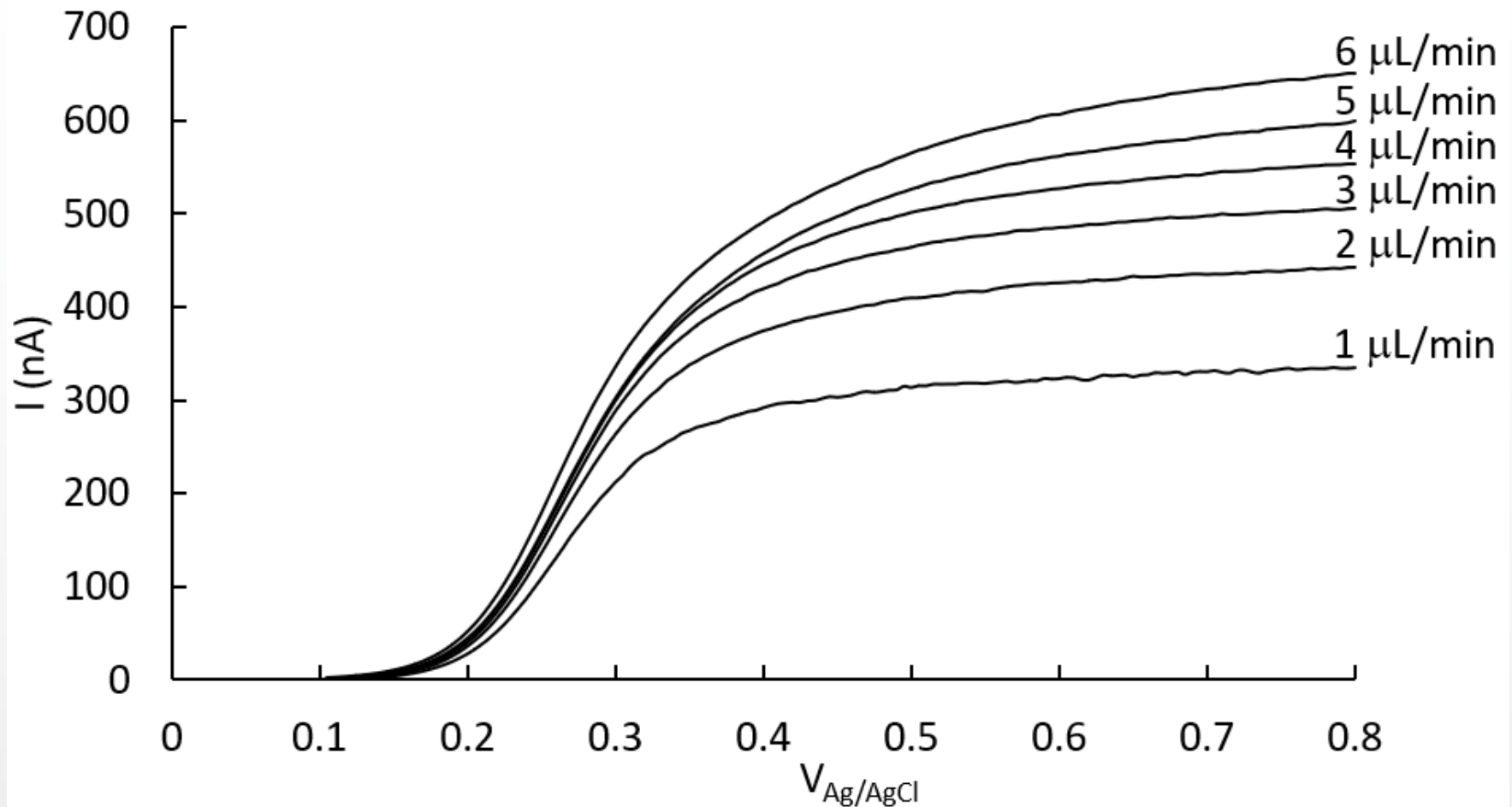


## Installed electrode butted flush against the channel



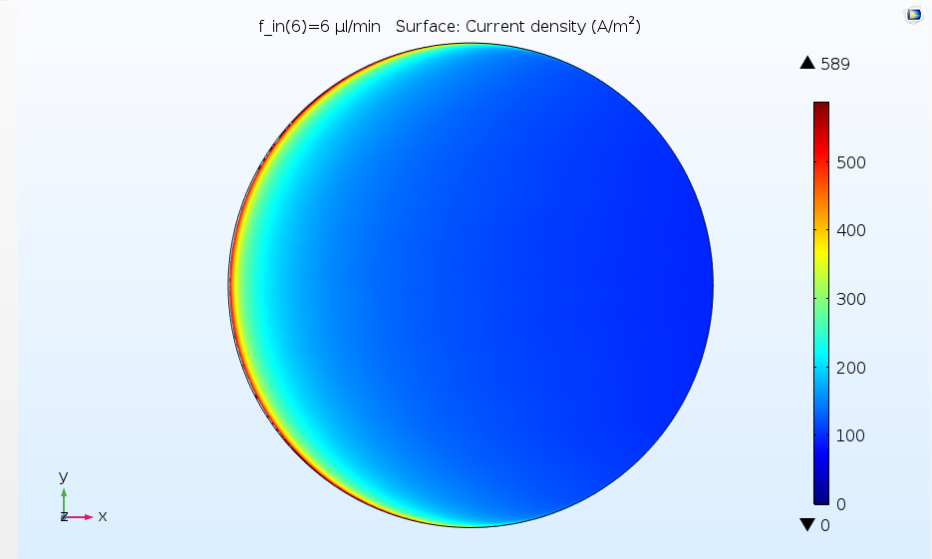
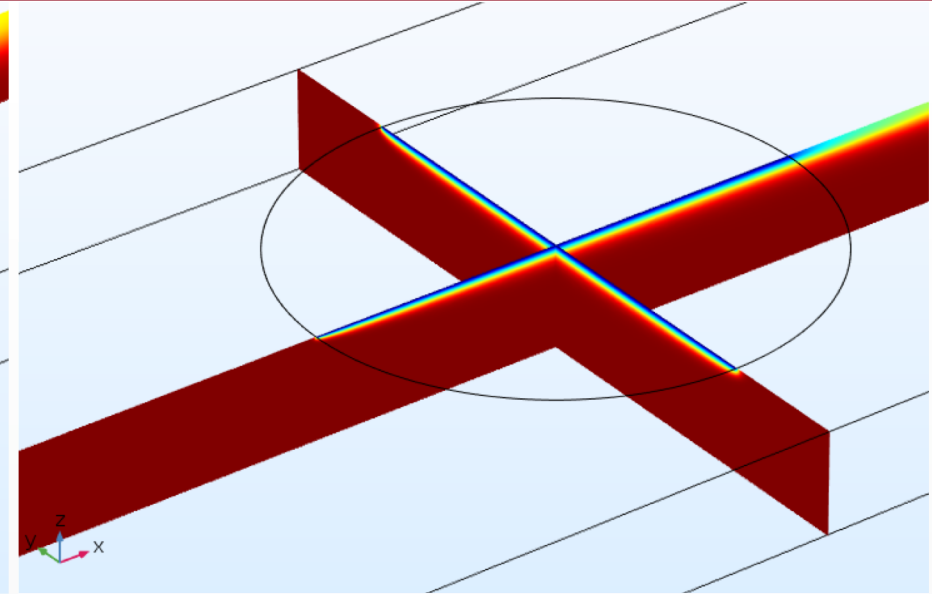
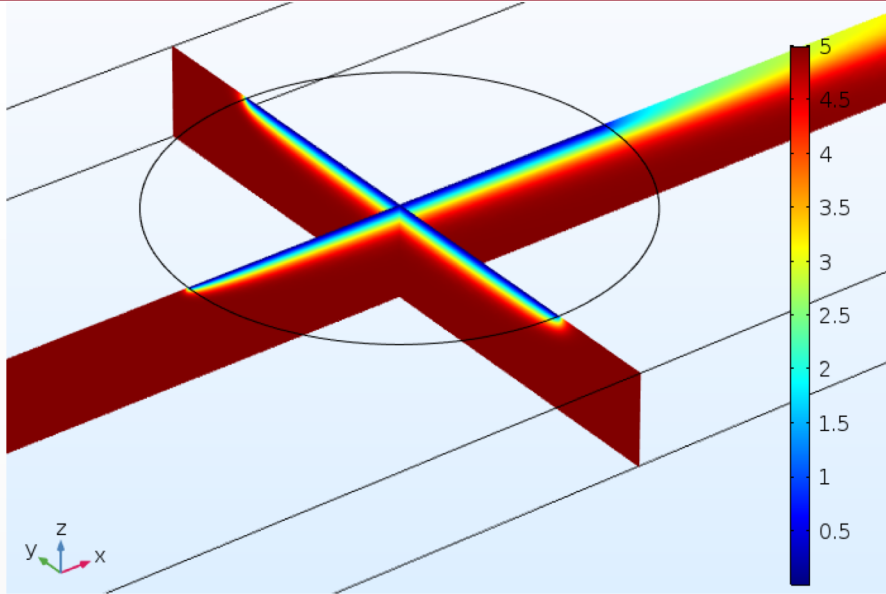


## Linear Sweep Voltammetry





# COMSOL Multiphysics® Final Elements Modeling



Oxidation of 20 mM  $K_4Fe(CN)_6$  in microfluidic chip at 1 and 6  $\mu\text{L}/\text{min}$



# Hydrodynamic Electrochemical Experiments

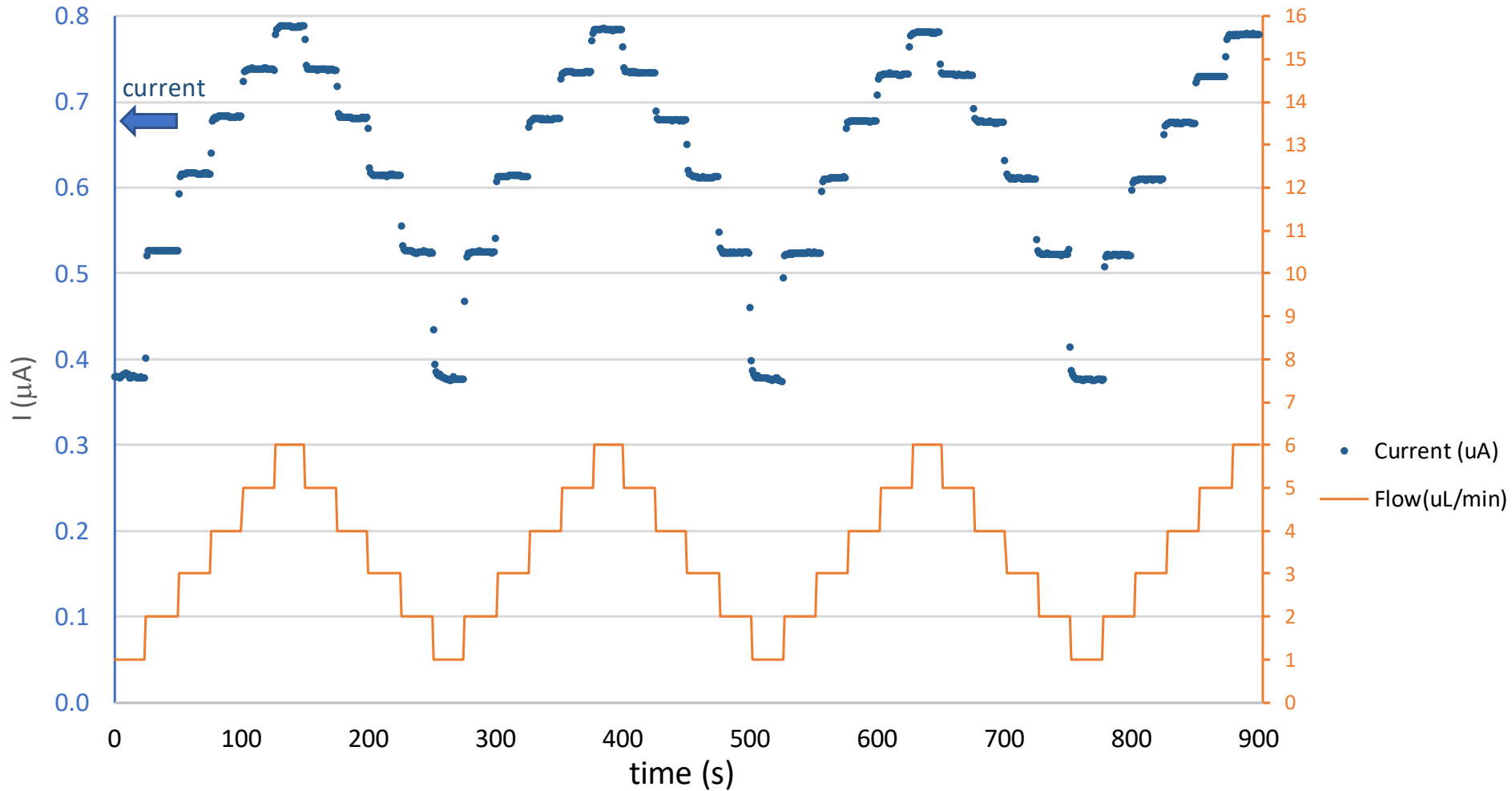


Figure 2. Chronoamperometry at different flows in microfluidic chip (WE@anodic potential of  $+0.5V_{\text{Ag}/\text{AgCl}}$ . Solution: 5 mM  $\text{K}_4\text{Fe}(\text{CN})_6$  (0.5 KCl electrolyte)



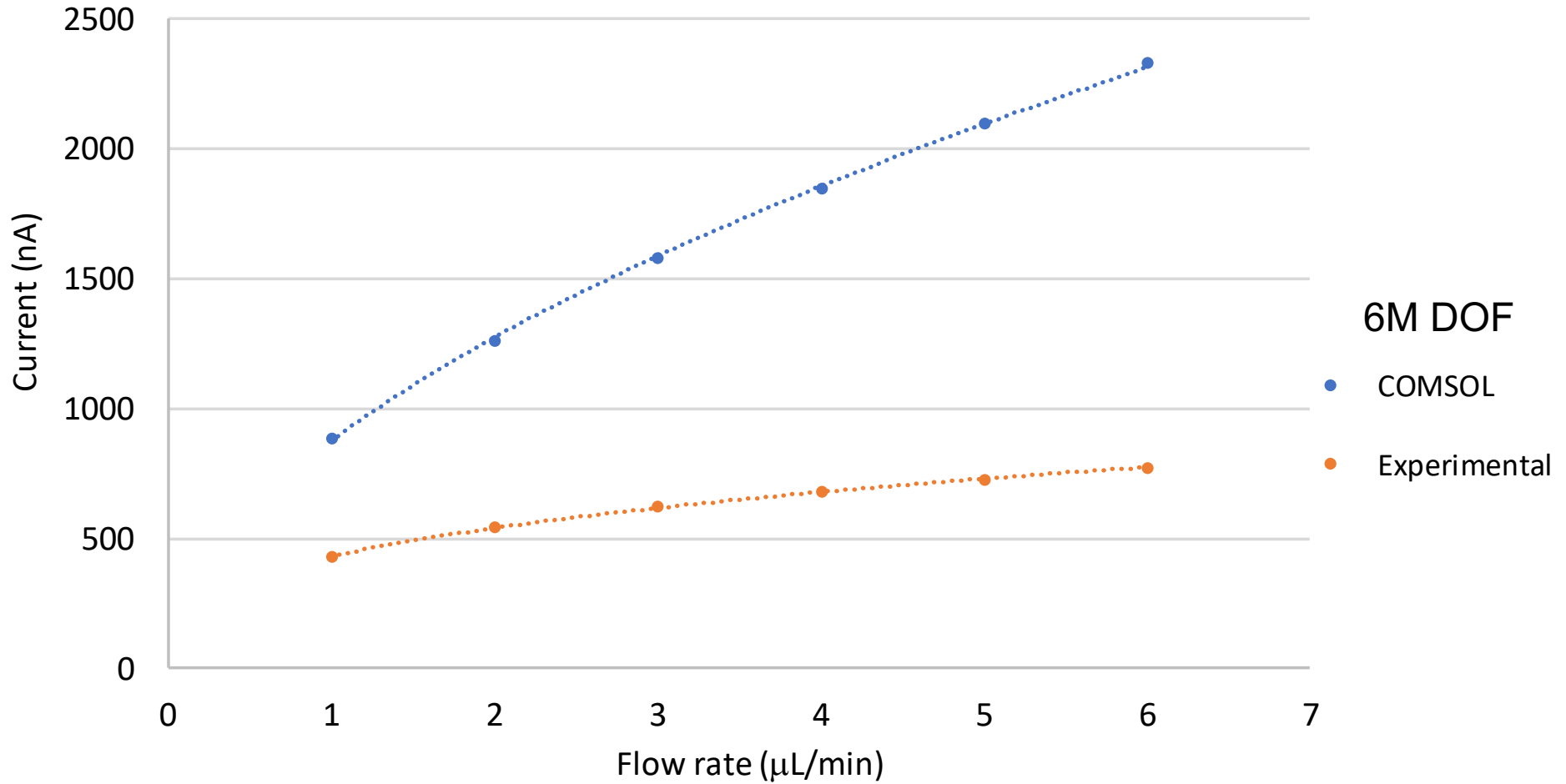


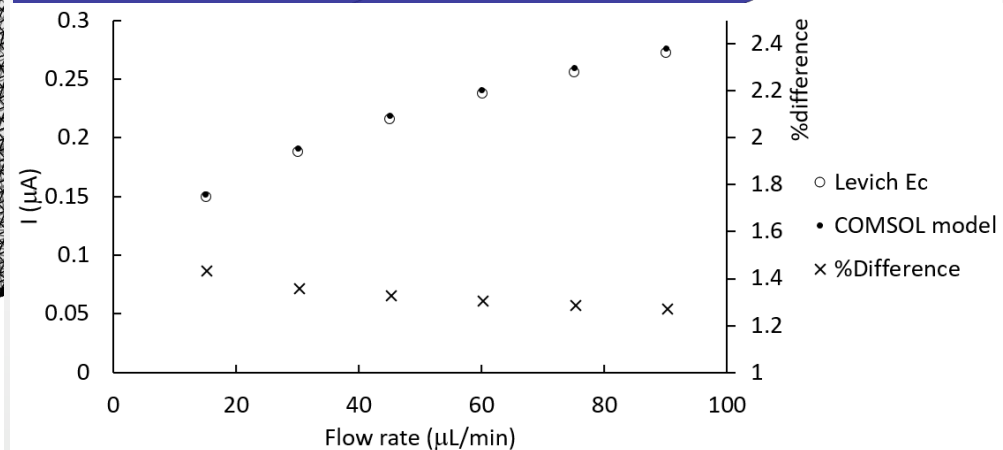
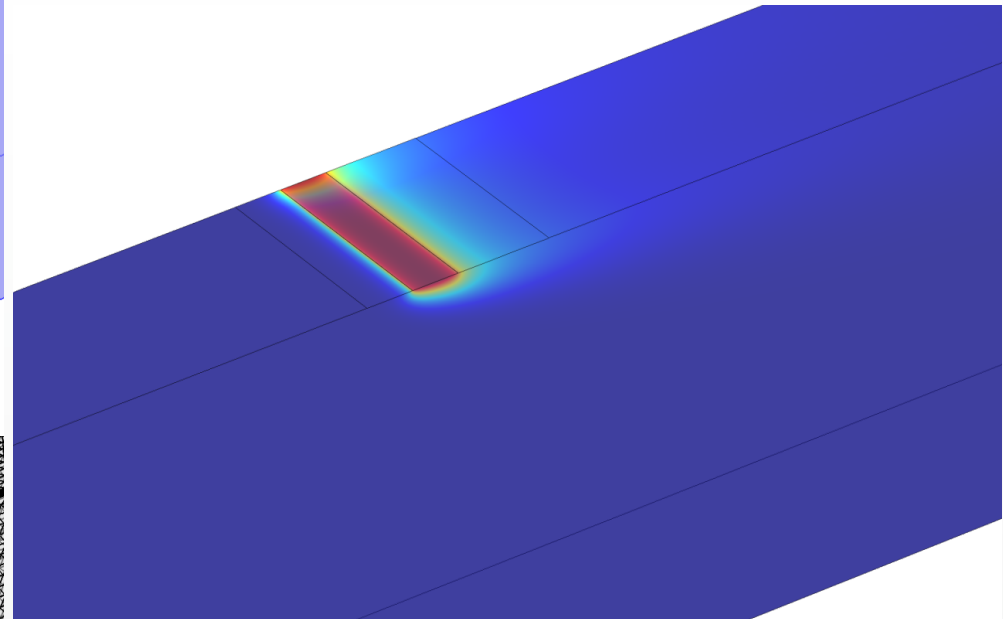
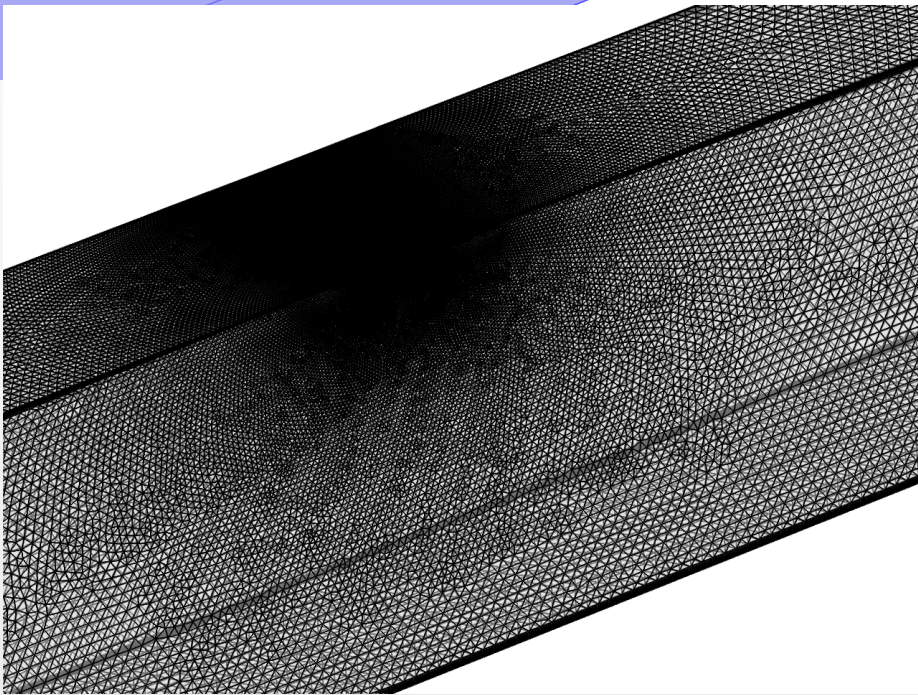
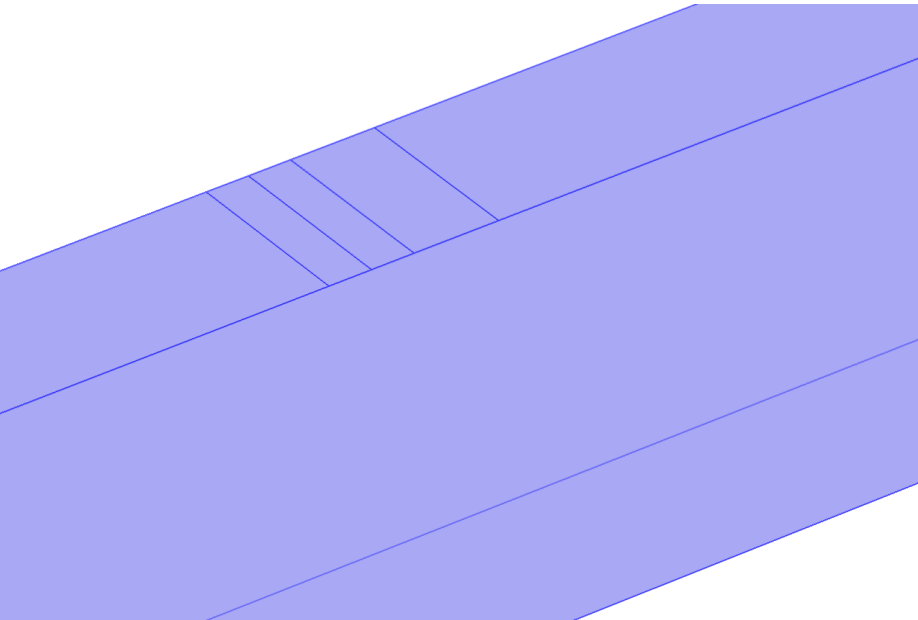
Figure 6. Limiting current at different flows for oxidation of 5mM  $K_4Fe(CN_6)$  in microfluidic chip



# Model Validation

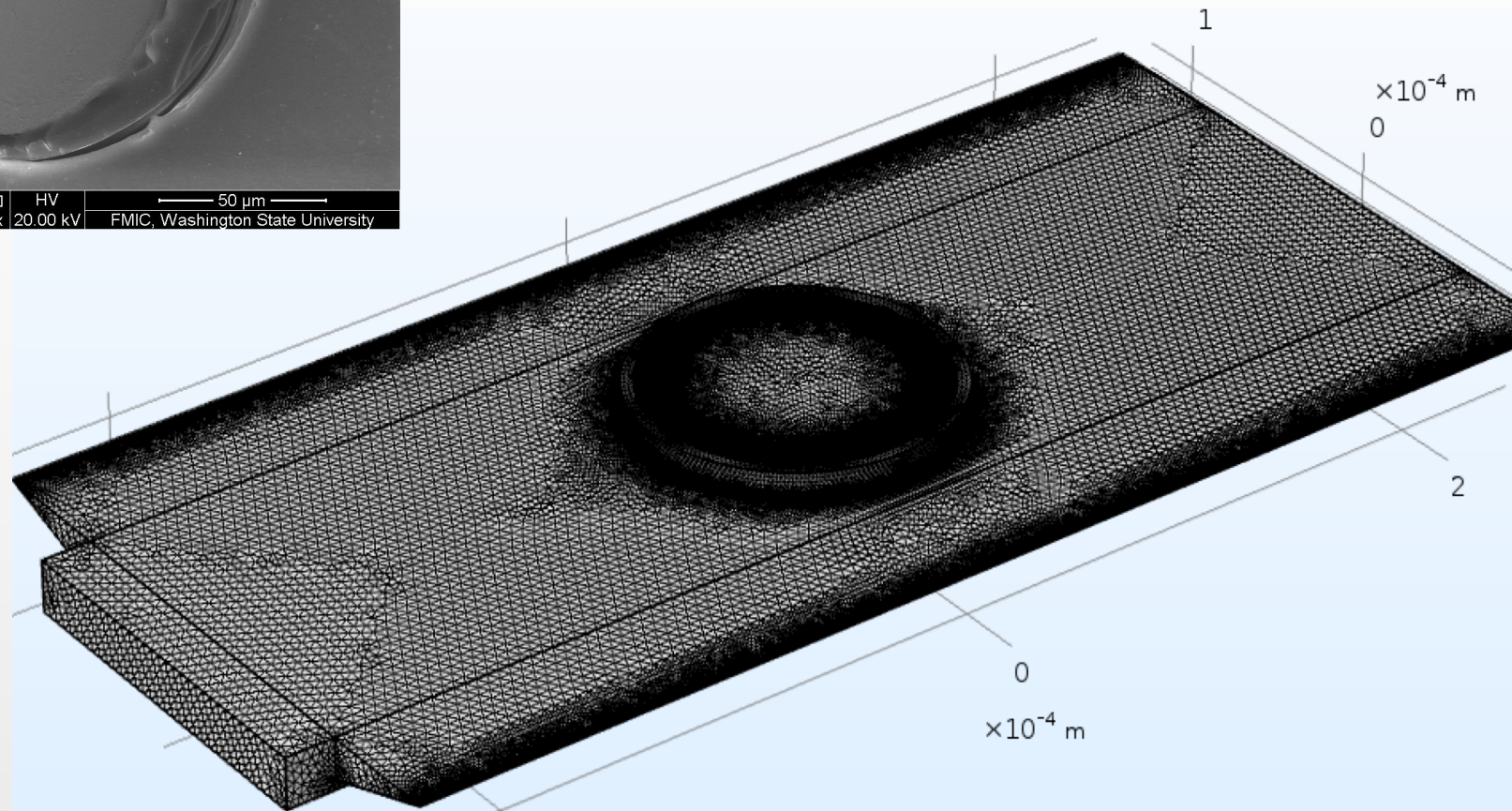
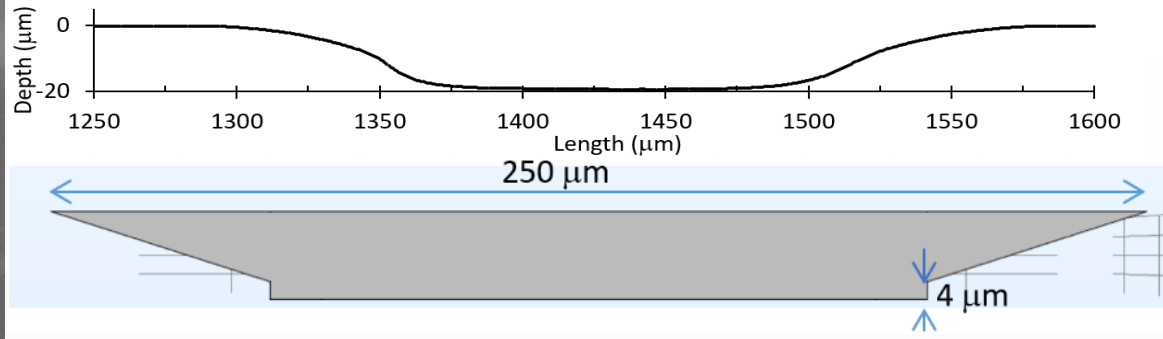
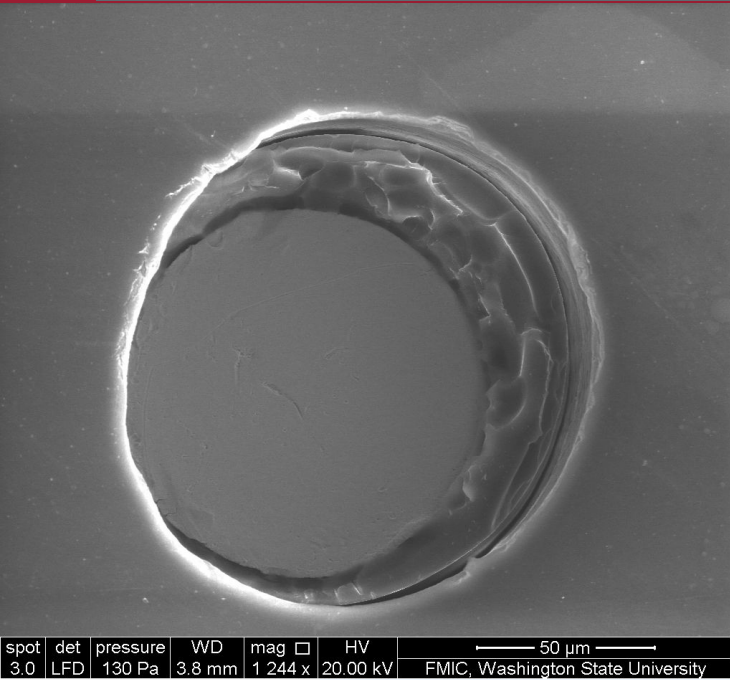
## The Levich Equation (Analytical)

$$I = 0.925 FWC_{red} (2L_e D_{reduced})^{\frac{2}{3}} \left( \left( \frac{8}{3} \right) \frac{v_{max}}{H} \right)^{\frac{1}{3}}$$



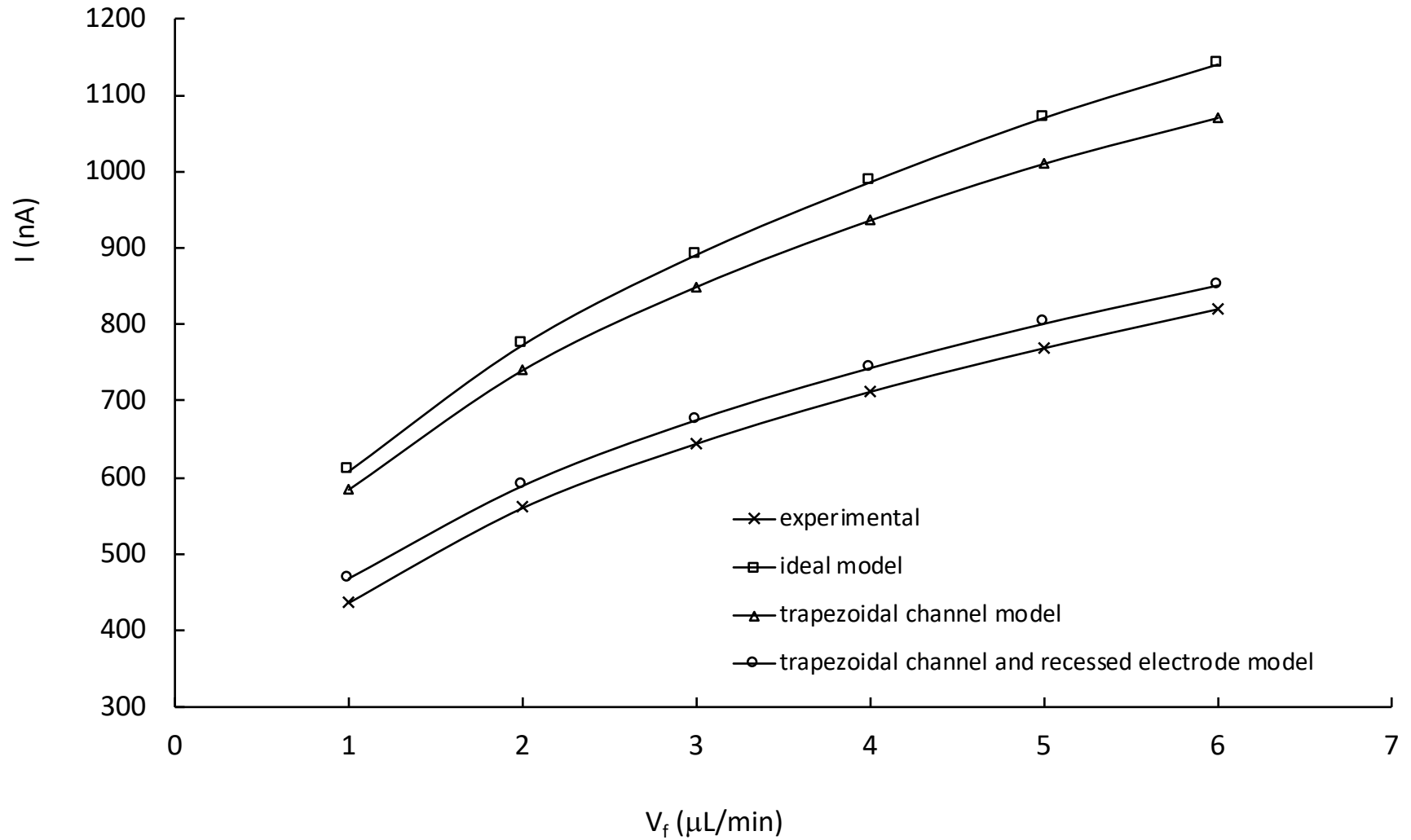


# Electrode and Channel Defects





# Effect of Defects on Simulation Current



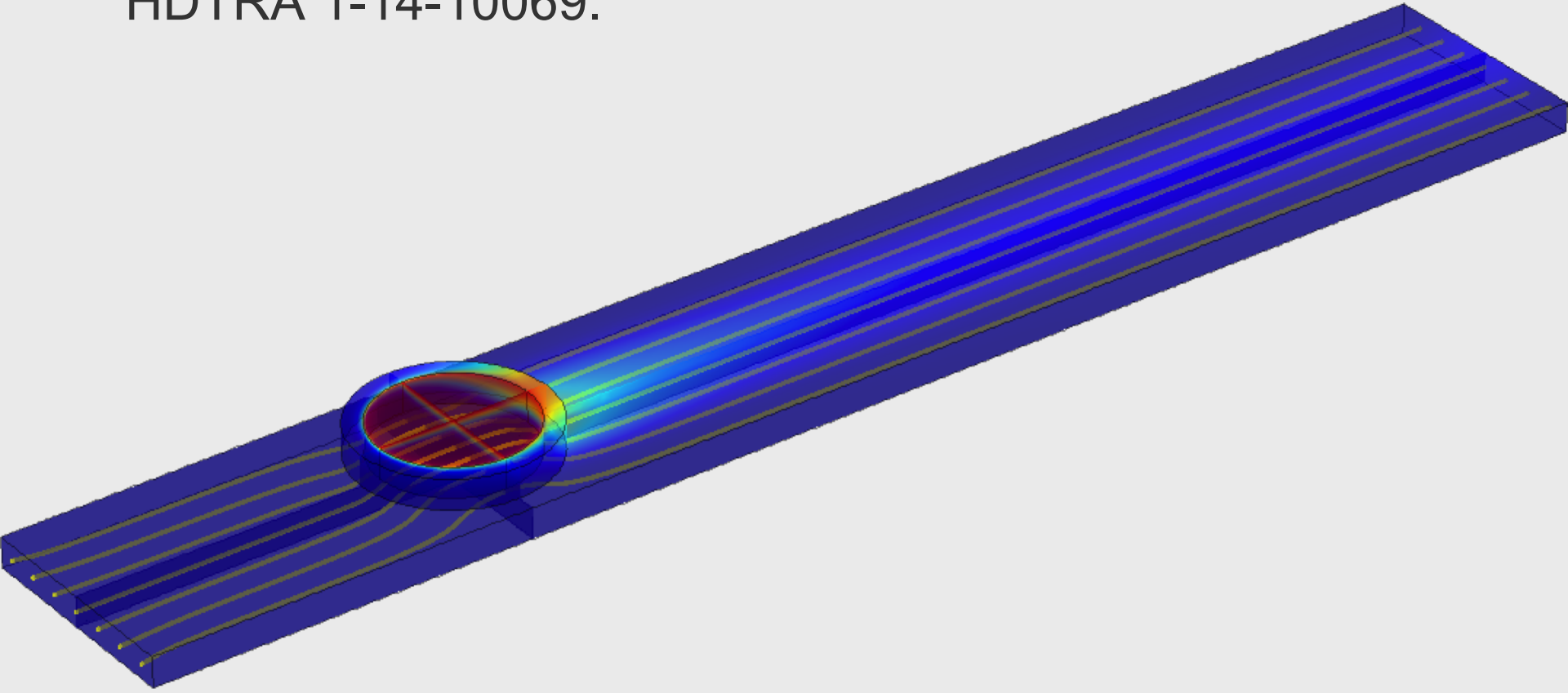


# Conclusions and Future Work

- 3D channel electrodes can be modeled using finite-element software COMSOL Multiphysics<sup>®</sup> to accurately predict limiting currents.
- Geometrical defects can be accounted for in the simulation of experiments.
- Future work: Electrochemical concentration of Ln/An from trace sources.

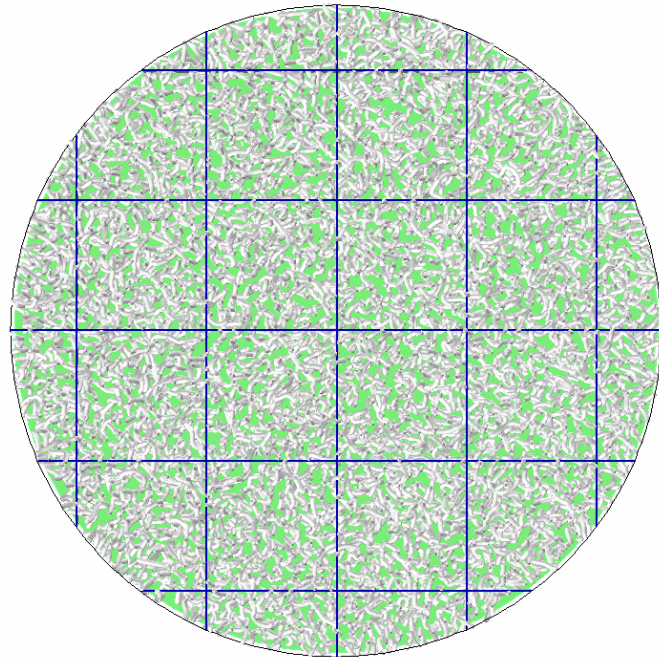
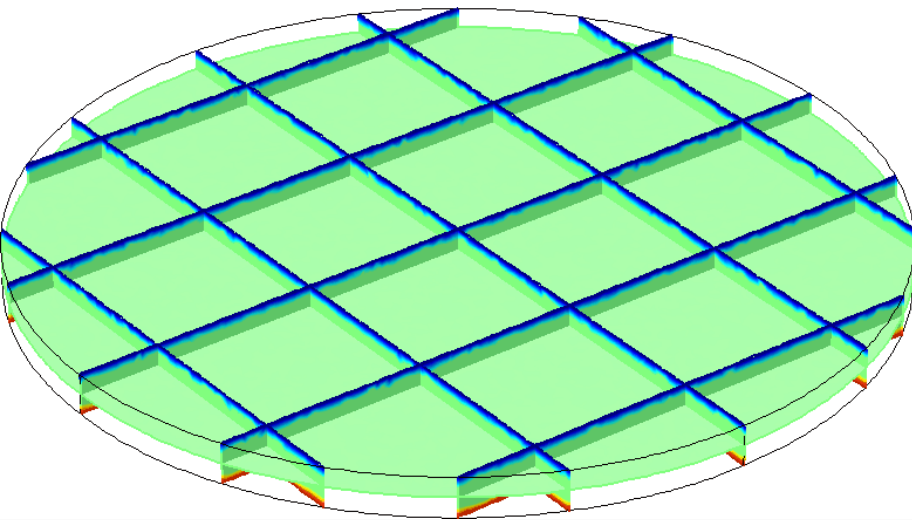
# Acknowledgement

- The material presented here is based on work supported in part by the U.S. Department of Defense under Award N° HDTRA 1-14-10069.





# Questions?



## COMSOL Illustrated Using COMSOL Multiphysics® 2018 Boston

Cornelius F. Ivory  
Voiland School of Chemical Engineering and Bioengineering  
Washington State University, Pullman WA, 99163



WASHINGTON STATE  
UNIVERSITY

**INTRODUCTION:** COMSOL Multiphysics® has proved invaluable for teaching "Transport Phenomena" to graduate and undergraduate engineers. This software allows us to visualize and explore solutions well beyond what could be done with pencil and paper. One of the topics that had previously been skipped, due to the complexity of the mathematics, was hydrodynamic instabilities. Using COMSOL, students are able to locate the point of neutral stability and then visualize changes in the system as the instability emerges, amplifies itself and then progresses to a secondary state.

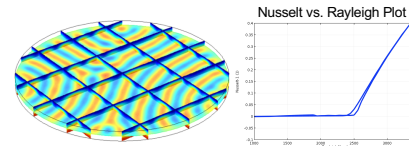


**Figure 1. Left:** Buoyancy-induced instability<sup>1</sup> in a thin film of water with the no-slip condition applied on all container surfaces and with surfaces heated from below, cooled from above and insulated on the sides. This system was modeled using equations [1-3].

**Right:** Nusselt number vs Rayleigh number plot showing the emergence of a secondary heat transfer mechanism near Ra=2500.

**COMPUTATIONAL METHODS:** All of the secondary flows shown in this poster were generated using some combination of the following equations as indicated in each figure caption. [1] the Navier-Stokes equation, [2] the Continuity equation, [3] the Thermal Energy equation and [4] the charge conservation equation.<sup>2</sup>

$$\rho \frac{\partial \mathbf{u}}{\partial t} + \rho \mathbf{u} \cdot \nabla \mathbf{u} = -\nabla p + \nabla \cdot \mu \nabla \mathbf{u} + \rho \mathbf{g} \quad [1]$$

$$\frac{\partial \rho}{\partial t} + \nabla \cdot \rho \mathbf{u} = 0 \quad [2]$$

$$\rho C_p \frac{\partial T}{\partial t} + \rho C_p \mathbf{u} \cdot \nabla T = \nabla \cdot k \nabla T + \sigma \mathbf{E} \cdot \mathbf{E} \quad [3]$$

$$\frac{\partial q}{\partial t} + \nabla \cdot \sigma \mathbf{E} = 0 \quad [4]$$

These bulk equations were solved together with the "no-slip" condition and with prescribed heat fluxes applied on all solid boundaries. The charge conservation equation assumed constant electrical conductivity, fixed potentials on the anode and cathode with all other surfaces electrically insulating. In all cases the initial conditions specified zero velocity and uniform temperatures throughout the computational domain.

**ACKNOWLEDGEMENT:** This work was supported in part by the Paul M. Hohenschuh Distinguished Professorship in Chemical Engineering awarded to Prof. Ivory in 2011.

**RESULTS:** Fig. 2 shows the secondary (left) and tertiary (right) flows that develop in a Couette viscometer when the dimensionless rotation rate, as characterized by the Taylor number, exceeds a first (left) and then a second (right) critical value.

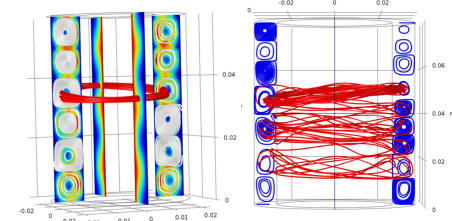


**Figure 2. Left:** Centrifugal instability<sup>3</sup> showing steady Taylor vortices formed in the annulus between a rotating inner cylinder and a fixed outer cylinder when the rotation rate exceeds a critical RPM.

**Right:** An oscillatory instability appears after a second critical Taylor number is reached. The flow is still laminar here so simulation is possible. This system was modeled using equations [1-2].

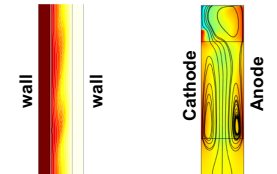


**Figure 3. Left:** Buoyancy instability showing roll vortices in a Clusius-Dickel column<sup>2</sup> heated on the right and cooled on the left. This system was modeled using equations [1-3].

**Right:** Oscillatory instability in a continuous flow electrophoresis device with Joule heating. This system was modeled using equations [1-4].

**CONCLUSIONS:** Transport instabilities that can be modeled using the equations of conservation can be readily simulated using COMSOL Multiphysics v5 so long as the secondary state is laminar. Generally, these simulations take less than an hour to set up; they run to completion in 10s of minutes for 2D problems or several hours for 3D problems, depending on their complexity.

### REFERENCES:

1. Chandrasekhar, S., Hydrodynamic and Hydromagnetic Stability, Dover Press, New York, 1961.
2. Bird, R. B., E. N. Lightfoot, and W. E. Stewart, Transport Phenomena, Revised 2<sup>nd</sup> Edition, John Wiley and Sons, N.Y. 2007.
3. Drazin, P. G. and W. H. Reid, Hydrodynamic Stability, Cambridge University Press, Cambridge 1981.

